Mesoporous $ZnFe_2O_4$ prepared through hard template and its acetone sensing properties

Yinglin Wang, Fangmeng Liu, Qiuyue Yang, Yuan Gao, Peng Sun, Tong Zhang, Geyu Lu

www.elsevier.com

PII: S0167-577X(16)31193-4
DOI: http://dx.doi.org/10.1016/j.matlet.2016.07.099
Reference: MLBLUE21227

To appear in: *Materials Letters*

Received date: 3 June 2016
Revised date: 19 July 2016
Accepted date: 19 July 2016

Cite this article as: Yinglin Wang, Fangmeng Liu, Qiuyue Yang, Yuan Gao, Peng Sun, Tong Zhang and Geyu Lu, Mesoporous $ZnFe_2O_4$ prepared throug hard template and its acetone sensing properties, *Materials Letters* http://dx.doi.org/10.1016/j.matlet.2016.07.099

Mesoporous $ZnFe_2O_4$ prepared through hard template and its acetone sensing properties

Yinglin Wang [a, b], Fangmeng Liu [b], Qiuyue Yang [b], Yuan Gao* [b], Peng Sun [b], Tong Zhang [b] and Geyu Lu* [a, b]

[a] State Key Laboratory of Automotive Simulation and Control, Jilin University, 2699 Qianjin Street, Changchun 130012, China

[b] State Key Laboratory on Integrated Optoelectronics, College of Electronic Science and Engineering, Jilin University, 2699 Qianjin Street, Changchun 130012, China.

Abstract

Mesoporous $ZnFe_2O_4$ with ordered tunnel and large specific surface area has been successfully prepared through hard template (mesoporous silica KIT-6). The necessary characterizations such as X-ray diffraction (XRD), Brunauer-Emmet-Teller (BET), transmission electron microscopy (TEM) and X-ray photoelectron spectroscopy (XPS) have been carried out to investigate the obtained material. $ZnFe_2O_4$ with mesoporous structure presents excellent crystallinity and periodic mesostructure. The sensing properties of gas sensor based on $ZnFe_2O_4$ mesoporous material towards acetone has been investigated. The sensor presents outstanding sensitivity, selectivity and longtime stability. This indicates that the obtained mesostructured $ZnFe_2O_4$ through hard template method is a potential acetone gas sensor material.

Key words: $ZnFe_2O_4$, hard template, mesoporous, acetone, gas sensor

*Corresponding author: Tel.: +86 431 85168384; fax: +86 431 85167808.

Email: gaoyuan@jlu.edu.cn (Y. Gao), lugy@jlu.edu.cn (G. Lu).

1. Introduction

Gas sensor based on metal oxide semiconductor (MOS) has attract significant attention recently as

simple and low cost devices to detect harmful volatile organic compounds (VOC) gases. Some promising sensing MOS materials [1-2] have been reported applied in gas sensors, such as SnO_2, ZnO and $ZnFe_2O_4$. Among them above, ferrites have been applied in gas sensor fabrication as the sensing material because they sometimes present more sensitive and stable performances for particular gas than other n-type MOS. Zinc ferrite ($ZnFe_2O_4$), as a typical ferrite spinel, has received tremendous interests for applied in many fields, including photocatalysis, information storage, and gas sensing [3, 4]. Moreover, numerous efforts have been devoted to synthesize $ZnFe_2O_4$ materials with different structures such as microspheres, nanotube and nanorods [5-7]. Especially, sensing materials with mesoporous structure can enhance the gas sensing properties for the large surface area and surface permeability [8]. Thus, the synthesis of $ZnFe_2O_4$ with mesoporous is extremely significant in plenty of applications.

In our present work, a facile synthesis route was applied in producing mesoporous $ZnFe_2O_4$ for acetone detection. Through hard template method, an ordered mesostructured $ZnFe_2O_4$ has been obtained with large specific surface area of 103.6 m^2 g^{-1} and average pore diameter about 8 nm. Various characterizations were carried out to investigate the morphology and chemical state of the obtained material. The gas sensors fabricated by our $ZnFe_2O_4$ sensing material presented good sensing performance toward acetone. The sensitivity of gas sensor to 100 ppm acetone reaches 11.6 at its optimum operating temperature of 225°C.

2. Experimental

All the chemical reagents used in the experiments were obtained from commercial sources (Sigma Aldrich) as guaranteed-grade reagents and were without further purification.

The mesoporous $ZnFe_2O_4$ was prepared by hard template route, ferric nitrate and zinc nitrate acted

as ferric and zinc precursor, respectively. 5.6 mmol of $Zn(NO_3)_2{\cdot}6H_2O$ and 5.6 mmol of $Fe(NO_3)_3{\cdot}9H_2O$ were dissolved into the mixture of 2.8 mmol of citric acid and 25 mL of ethanol under continuous stirring for 30 min. After adding1.0 g of KIT-6, the obtained slurry was stirred at 40°C till all the solvent was evaporated further followed by calcination at 450°C for 2 h. Finally, the obtained nanoparticles was dissolved in NaOH (2 mol/L) for 12 h to remove KIT-6. The as-prepared slurry was washed and centrifuged with ethanol and DDI, and dried at 80°C.

The crystallinity and phase of the sensor materials were characterized by X-ray diffraction (XRD, Rigaku D/MAX-2550, λ = 0.15418 nm). N_2 adsorption-desorption isotherms and the pore size distribution were measured with a Micrometrics Gemini VII surface area and porosity system. The samples were degassed at 200°C prior to the BET measurement. The surface morphology was investigated by scanning electron microscopy (SEM, JEOL JSM-7500F).Transmission electron microscopy (TEM) and high resolution transmission electron microscopy (HRTEM) characterizations were performed with a JEOL TEM-2100 instrument. X-ray photoelectron spectroscopy (XPS) was carried out at room temperature on Thermo ESCALAB 250 spectrometer.

The sensor was fabricated in accordance with the literature [9]. The gas sensing properties were measured with a RQ-2 static characterization system. The gas response was defined as $S = R_a/R_g$, where R_a and R_g were the resistance in air and the target gas, respectively. In addition, the response time was defined as the time required for the gas response to reach 90% of the final equilibrium value after test gas was injected.

3. Results and discussion

3.1 Structure and morphology characteristics

The XRD patterns of as-prepared mesoporous $ZnFe_2O_4$ is presented in Fig, 1(a). As depicted from

the inset, the low-angle XRD pattern of $ZnFe_2O_4$ with a sharp diffraction peak of (211) accordance with silica template KIT-6. The peaks of as-prepared sample happened at the same degree with KIT-6 indicates the successful replication from the mesoporous structure of the hard template. From the wide-angle XRD patterns, all the recorded diffraction peaks have been well indexed to the pure cubic phase of spinel $ZnFe_2O_4$ (JCPDS card No. 77-11) with lattice constant of a = 8.429 Å. Furthermore, no diffractions indexed impurities have been found and indicates the high purity of the sample.

The nitrogen adsorption-desorption isotherm and pore sized distribution of $ZnFe_2O_4$ are shown in Fig. 1(b) and inset. The typical type IV Brunauer isotherm with a capillary condensation occurs in the relative pressure (P/P_0) of 0.5-1.0. H1 hysteresis loop identified as the typical characteristic of mesostructure can also be observed. The pore size distribution curve reveals two peaks center at about 3.8 nm and 8.2 nm, respectively. The peak occurs at 3.8 nm is tensile strength effect (TSE) peak which can be neglect. The BET surface area of $ZnFe_2O_4$ is calculated to be 103.6 $m^2 g^{-1}$. Such a large specific surface area and mesoporous structure benefit chemical reaction and diffusion of detected gas.

Fig. 1

Detailed mesostructured features of $ZnFe_2O_4$ are further investigated by SEM and TEM. The as-prepared sample with distinguishable ordered mesostructure is shown in Fig. 2(a). The HRTEM image inset presents the clear well developed lattice fringes, and the crystallographic planes (311) of spinel $ZnFe_2O_4$ (JCPDS card No. 77-11) is observed with the corresponding lattice of 0.257 nm. The pore size is observed as about 8 nm in Fig. 2(b), which is matched with the BET result.

Fig. 2

The composition and the chemical state of the elements are performed by XPS. Fig. 2(c) reveals the as-prepared materials are obviously composed of Zn, Fe and O. Two fitting peaks with binding

energy values of ~1045 and ~1022 eV exhibited in the Zn 2p spectrum in Fig. 2(d) could be attributed to Zn $2p_{1/2}$ and Zn $2p_{3/2}$, respectively [10]. As Fe 2p spectrum exhibited in Fig. 2(e), the binding energy peaks for Fe $2p_{3/2}$ at ~713.6 and ~711.5 eV correspond well with the tetrahedral site (A site) and octahedral (B site), respectively [11]. In addition, the peak occur at the binding energy of ~725.6 eV is well consistent with Fe $2p_{1/2}$ and the other residual peaks present the shakeup satellite structure. The high resolution XPS spectrum of O 1s could be resolved to two Gaussian function peaks with the energy of ~530.6 and ~532.2 eV in Fig. 2(f). The peak at ~530.6 eV could be assigned to the lattice oxygen and the other is the adsorbed oxygen species. The surface absorbed oxygen species play a significant role in the enhancing gas performance as they are capable of reacting with detected gas.

3.2 Gas sensing performances

The black dot-line curve shown in Fig. 3(a) reveals the variation sensitivity of the sample to 100 ppm acetone with the increasing operation temperature. The response curve present bell-shape in the range of 175 - 300°C, and the response to 100 ppm acetone is 11.6 at the optimum operation temperature of 225°C. The red dot-line pattern in Fig. 3(a) depicts the variation in response time of mesoporous $ZnFe_2O_4$ as a function of temperature towards 100 ppm acetone. The response time decreases with increasing in temperature, which is attributed to the fast adsorption and desorption of gas molecules on the material surface at higher temperature.

.Fig. 3

The long-term stability of mesoporous $ZnFe_2O_4$ has been investigated by testing 100 ppm acetone for 28 days, which is shown as blue dot-line curve in Fig. 3(b). All of the response values almost unchanged during the test which demonstrate the excellent stability of the sensor. The selectivity of mesoporous $ZnFe_2O_4$ to 100 ppm of different detected gases is carried out in red bar of Fig. 3(b).

Compared with acetone, the sensor present lower response to ethanol, methanol, toluene and almost no response to other gases. Therefore, the gas sensor based on mesoporous $ZnFe_2O_4$ reveals an outstanding selectivity toward acetone. The comparison with other $ZnFe_2O_4$ nanostructures has been illustrated in Table s1†.

Sensing mechanism of $ZnFe_2O_4$ is based on the change in resistance of the sensor by the adsorption and desorption process of oxygen molecules on the surface of material. In air atmosphere, oxygen molecules adsorb on the surface of mesoporous $ZnFe_2O_4$, which would capture free electrons from the conduction band and form adsorbed oxygen species ($O_2^-{}_{ads}$, $O^-{}_{ads}$, $O^{2-}{}_{ads}$). It leads to the decrease of electrons concentration and the increase of the resistance of the sensor. When the sensor exposed to acetone, the acetone gas molecules would react with the adsorbed oxygen species which is shown as follow:

$$C_3H_6O + 8O^-{}_{ads} \rightarrow 3CO_2 + 3H_2O + 8e^- \quad (1)$$

This process releases the captured electrons back to the conduction band of $ZnFe_2O_4$ which finally leads to the lower resistance of the sensor.

4. Conclusion

In this work, hard template KIT-6 with mesostructure was employed in fabricating the mesoporous $ZnFe_2O_4$. The as-prepared materials presented order mesotructure with uniform pore size of ~8 nm and high specific surface area of 103.6 $m^2\ g^{-1}$ which are beneficial for gas diffusion and provide more active sites. The gas sensor with the obtained $ZnFe_2O_4$ exhibits excellent sensing performance towards acetone, which demonstrates the mesoporous $ZnFe_2O_4$ is an excellent candidate for acetone gas sensing.

Acknowledgments

This work was supported by the National Nature Science Foundation of China (61304242), Science and Technology Development Program of Jilin Province (No.20150520091JH).

References

[1] J. S. Jang, S. J. Kim, S. J. Choi, N. H. Kim, M. Hakim, A. Rothschild, I. D. Kim. Nanoscale 7 (2015) 16417-16426.

[2] X. Zhou, B. Wang, H. Sun, C. Wang, P. Sun, X. Li, X. Hu, G. Lu. Nanoscale 4 (2012) 194-205.

[3] H. Zhu, X. Gu, D. Zuo, Z. Wang, N. Wang, K. Yao. Nanotechnology 19 (2008) 405503.

[4] Y. Fu, X. Wang. Ind. Eng. Chem. Res. 50 (2011) 7210-7218.

[5] Z. Li, X. Lai, H. Wang, D. Mao, C. Xing, D. Wang. J. Phys. Chem. C 113 (2009) 2792-2797.

[6] F. Liu, X. Li, Q. Zhao, Y. Hou, X. Quan, G. Chen. Acta Mater. 57 (2009) 2684-2690.

[7] N. Wang, H. Xu, L. Chen, X. Gu, J. Yang, Y. Qian. J. Power Sources 247 (2014) 163-169.

[8] P. Song, D. Han, H. Zhang, J. Li, Z. Yang, Q. Wang. Sens. Actuators B: Chem. 196 (2014) 434-439.

[9] Y. Wang, X. Cui, Q. Yang, J. Liu, Y. Gao, P. Sun, G. Lu. Sens. Actuators B: Chem. 225 (2016) 544-552.

[10] R. Sahoo, S. Santra, C. RayRay, A. Pal, Y. Neqishi, S. K. Ray, T. Pal. New J. Chem. 40 (2016) 1861-1871.

[11] J. Zhang, J. Song, H. Niu, C. Mao, S. Zhang, Y. Shen. Sens. Actuators B: Chem. 221 (2015) 55-62.

Figure captions

Fig. 1. (a) XRD patterns and (b) BET curves of obtained mesoporous $ZnFe_2O_4$.

Fig. 2. (a) SEM image (HRTEM inset), (b) TEM image and (c) XPS spectra of the as-prepared $ZnFe_2O_4$; the XPS curves of (d) Zn2p, (e) Fe2p and (f) O1s.

Fig. 3. (a) Gas response and response time curves towards operation temperature, (b) long-term stability and selectivity of $ZnFe_2O_4$.

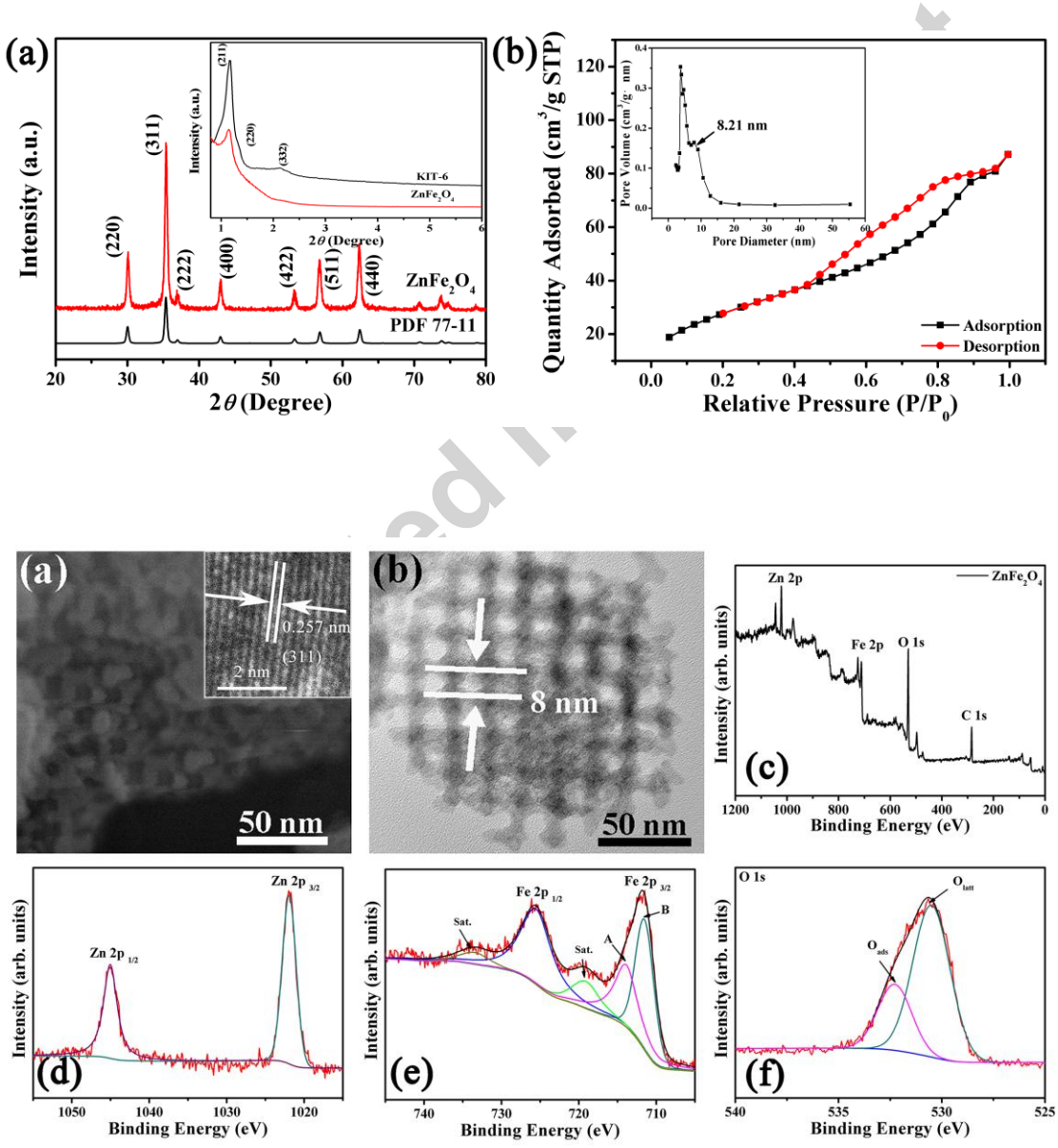

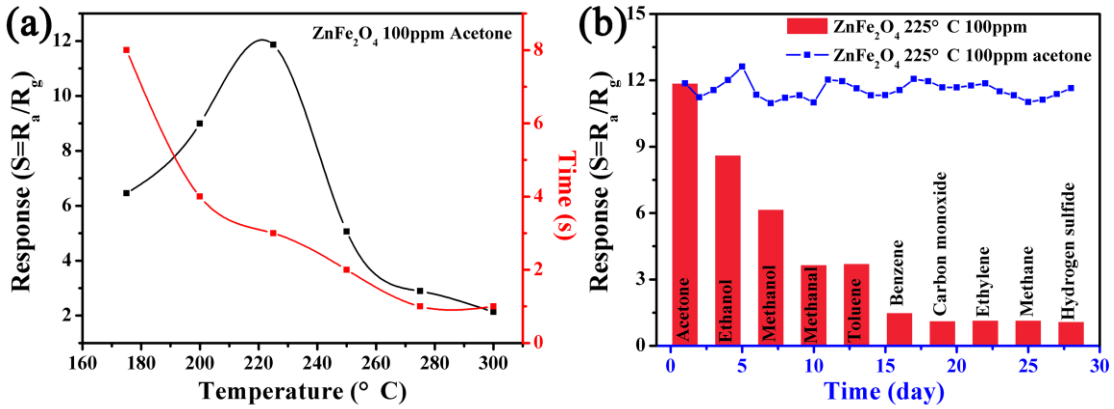

Highlights

1. $ZnFe_2O_4$ with ordered mesoporous structure has been successfully prepared by hard template (KIT-6).
2. The mesoporous $ZnFe_2O_4$ possesses the higher surface specific area and uniform pore size distribution.
3. The mesoporous $ZnFe_2O_4$ has been applied in gas sensor which has an outstanding sensing performance towards acetone.
4. We expect that the mesoporous $ZnFe_2O_4$ would be an excellent candidate for acetone gas sensing.